Computational Design of Reaction-Diffusion Patterns Using DNA-Based Chemical Reaction Networks

Neil Dalchau[1], Georg Seelig[2], and Andrew Phillips[1]

[1] Microsoft Research, Cambridge, CB1 2FB, UK
{ndalchau,aphillip}@microsoft.com
[2] University of Washington, WA, USA
gseelig@uw.edu

Abstract. DNA self-assembly is a powerful technology for controlling matter at the nanometre to micron scale, with potential applications in high-precision organisation and positioning of molecular components. However, the ability to program DNA-only self-organisation beyond the microscopic scale is currently lacking. In this paper we propose a computational method for programming spatial organisation of DNA at the centimetre scale, by means of DNA strand displacement reaction diffusion systems. We use this method to analyse the spatiotemporal dynamics of an autocatalytic system, a predator-prey oscillator and a two-species consensus network. We find that both autocatalytic and oscillating systems can support travelling waves across centimetre distances, and that consensus in a spatial context results in the spontaneous formation of distinct spatial domains, in which one species is completely eliminated. Together, our results suggest that programmed spatial self-organisation of DNA, through a reaction diffusion mechanism, is achievable with current DNA strand displacement technology.

Keywords: DNA strand displacement, autocatalysis, consensus, approximate majority, reaction-diffusion, oscillators, travelling waves.

1 Introduction

Biological systems rely on a variety of mechanisms for the organisation of matter across spatial scales. At the subcellular scale, molecular self-assembly is an efficient way of creating shapes and structures, for example to assemble viral capsids from protein building blocks [1]. To propagate signals over distances beyond the cellular scale, biological systems often rely on diffusible signalling molecules that interact with other molecular components to form reaction diffusion patterns [2]. For instance, a reaction diffusion mechanism was recently proposed to explain digit formation in mouse embryos [3].

In recent years, DNA nanotechnology has made spectacular progress in the structural self-assembly of micron-sized objects with nanometre scale precision

[4]. Even centimetre-length DNA crystals [5] and hydrogels [6] have been experimentally realised. However, these materials have relatively simple long-range order that is either periodic or random. To replicate the diversity and scale of biological organisms, novel approaches are needed that extend to the centimetre scale and beyond. A reaction diffusion mechanism based on DNA molecules diffusing through and reacting in a hydrogel or similar matrix could provide a promising solution.

There are several examples of chemical systems capable of pattern formation, most famously the Belousov-Zhabotinskii system [7]. One of the earliest examples of spatial organisation in a cell-free biochemical system is the travelling waves of *in vitro* evolving RNA observed by Bauer and co-workers [8]. More recently, Isalan *et al.* [9] engineered a cell-free transcription-translation system that mimicked the pattern forming program observed in *Drosophila*. Simpson *et al.* proposed a method for implementing amorphous computation with *in vitro* transcription networks [10]. Rondelez and co-workers elegantly demonstrated travelling wave patterns in a molecular predator prey model created using a combination of DNA molecules, nicking enzymes and polymerases [11]. However, all of these approaches rely on enzymes and are thus more sensitive to reaction conditions than an approach that uses DNA alone.

Ellington and co-workers took a first step towards demonstrating pattern formation with enzyme-free DNA strand displacement systems by engineering a DNA-based edge detection circuit [12, 13]. Using UV light, a target pattern was first projected onto a gel that contained multiple DNA reactants, some of which had photo-cleavable bases. This initial pre-patterning activated a reaction pathway that led to pattern refinement. Scalise and Schulman [14] developed a modelling framework based on reaction diffusion equations for generating arbitrary shapes and patterns, starting from a small set of localised DNA signal *sources*. In principle, transient wave patterns and even stable Turing patterns could emerge from homogeneous inital conditions with small random perturbations. If realised with DNA molecules, such emergent patterns could complement existing approaches for self-assembly or diffusible signalling based on pre-patterned information by providing a mechanism for initial symmetry breaking. To understand if such self-organised patterns are within reach of current DNA technology, we first investigate how information can propagate in simple DNA strand displacement systems with a single localised input source. Then, we investigate the behaviour of a multi-reaction network with homogeneous (but noisy) initial conditions.

Recent work demonstrated that it is possible, in principle, to build DNA components that can approximate the kinetics of any well-mixed chemical reaction network (CRN) [15–17]. CRNs were proposed as a prescriptive programming language for specifying a target behaviour, which is then realised with DNA components. Here, we propose to build on this work to go beyond well-mixed chemistry. In particular, we demonstrate that DNA molecules can be programmed to approximate the behaviour of chemical reaction diffusion systems that yield self-organising patterns with macroscopic dimensions.

Central to this work is the use of computer-aided design tools. The Visual DSD (vDSD) software uses a textual syntax to describe an initial set of DNA molecules, and automatically generates the corresponding strand displacement reactions [18, 19]. It has previously been used to aid the design of several DSD circuits [17, 20–22]. Here, we extend vDSD to enable simulations of reaction diffusion DSD systems in a range of spatially heterogeneous scenarios. We design systems that form spatial patterns and analyse their behaviour in the context of realistic kinetic parameters. We then propose a number of scenarios that could be tested experimentally. Specifically, we demonstrate the design of systems that generate periodic travelling waves and stationary patterns, and analyse the impact of leaks arising from dysfunctional DNA gates enabling us to identify key insights and constraints on our systems prior to their construction.

2   Methods

Two-Domain DNA Strand Displacement. We consider the implementation of high-level CRNs using DNA strand displacement, following the two-domain approach proposed in [16]. *Signal strands* are single-stranded DNA (ssDNA) molecules which combine a short *toehold* domain and a longer *recognition* domain. The recognition domain specifies the identity of a signal, while the toehold domain can be shared among multiple signals. Accordingly, we use the notation ⟨t x⟩ to represent a signal strand X. To implement the stoichiometry of an arbitrary chemical reaction in the two-domain scheme, a nicked double-stranded DNA (ndsDNA) *join* gate receives all reactant strands and produces a *translator* strand, which then triggers the release of product strands from a *fork* gate (see [16, 17] for a detailed description). We adopt a naming convention for join and fork gates in which subscripts identify the reactants and products respectively. For example, the reaction $B + X \rightarrow 2X$ is implemented by ⟨t b⟩ and ⟨t x⟩ strands binding Join_{BX} gates, with Fork_{2X} gates producing two ⟨t x⟩ strands.

Error Modes. We consider the impact of imperfections in DNA strand/gate synthesis, as modelled in [17]. Specifically, we consider a *leak* parameter, which is the fraction of ndsDNA gates that spontaneously produce their output strand without requiring inputs.

Simulating Partial Differential Equations (PDEs) in Visual DSD. To analyse the spatiotemporal dynamics of DNA strand displacement circuits, and to provide the means for others to do this conveniently, we incorporated numerical solvers for partial differential equations into the Visual DSD (vDSD) software. Specifically, we provide numerical algorithms to solve problems of the form

$$\frac{\partial c}{\partial t} = f(c) + D\nabla^2 c \tag{1}$$

where c is the vector of concentrations and D is the diagonal matrix of diffusion rates, and ∇^2 represents the second spatial derivative. Solvers for both 1- and

2- dimensional domains have been implemented, using a Crank-Nicolson finite difference approach [23]. Extensions to the DSD programming language enable specifying PDE solver parameters, by way of *directives* (see Appendix A[1] for a complete list; Table S1). A screenshot of the new PDE-solving capabilities of vDSD is shown in Fig. 1.
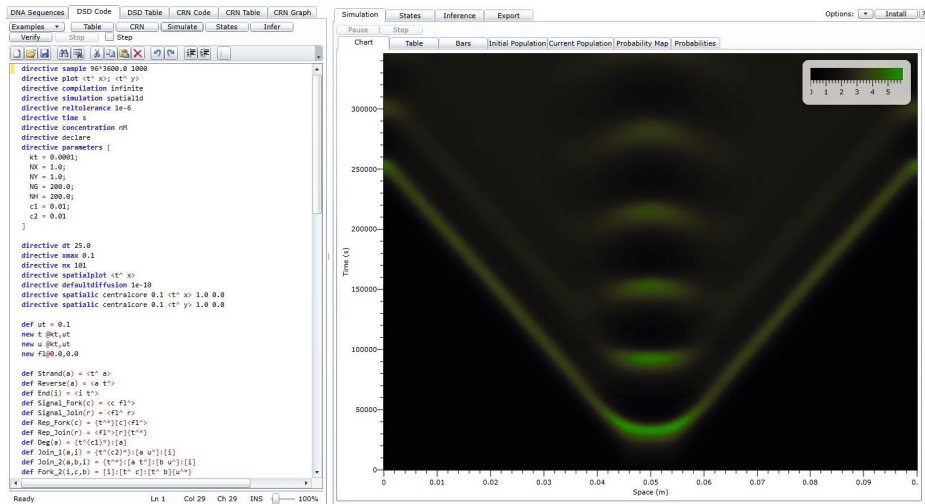

Fig. 1. Screenshot of the Visual DSD software during a 1d spatial simulation

Using the *defaultdiffusion* directive, we applied a diffusion rate of 10^{-10} m^2 s^{-1} for all ssDNA strands and dsDNA gates, as approximated in [24]. Note that when simulating reaction-diffusion equations, modifications to a uniform D (i.e. $D \mapsto \alpha D'$) can be applied by rescaling the spatial domain as $x \mapsto \sqrt{\alpha}x'$. Therefore, all qualitative behaviours presented here are independent of the choice of diffusion rate.

Simulation of an Invasion Scenario. To determine how local signals propagate through a reactive medium, we consider *invasion scenarios*. These occur when the initial concentrations of specified molecular species are non-zero only in some sub-region $\mathcal{R}$ of the full domain. In a vector of concentrations $c = c(x, t)$, where x is the position and t is the time, the elements c_I (where I is a subset of the species labels) have initial conditions

$$c_I(x,0) = \begin{cases} c_I^0 & \text{if } x \in \mathcal{R} \\ 0 & \text{otherwise} \end{cases} \tag{2}$$

In the case of DNA strand displacement, we supplied gates and auxiliary strands uniformly in space. In vDSD, the species in the subset I can be initialised

---

[1] Appendices in the online version, available from the author's website.

according to (2) with $\mathcal{R}$ as a central channel in 1d or a central square in 2d, by using the `centralcore` option of the `spatialic` directive (Table S1).

3   Results

To predict how DNA diffusion might enable pattern formation over macroscopic scales, we considered three circuits that have previously been well-studied at the CRN level: an autocatalytic circuit, a Lotka-Volterra predator-prey oscillator and a consensus network. We implemented DNA strand displacement versions of these circuits, and analysed their spatiotemporal dynamics with vDSD.

3.1   Wave Propagation in an Autocatalytic Circuit

One of the simplest known systems for which travelling wave phenomena have been observed is an autocatalytic reaction [25]

$$X + Y \xrightarrow{k} 2Y \tag{3}$$

The distance travelled in time t by the front of a travelling wave in an autocatalytic reaction-diffusion system is $d_W \approx 2\sqrt{fDt}$ [26], where f is the *intensity* of the interaction. In this case f becomes approximately equal to $k[X]_0$, where $[X]_0$ is the initial concentration of X (see Appendix B for a derivation). The diffusion coefficient of a single-stranded 20mer in water at 20°C was reported to be on the order of 10^{-10} m^2 s^{-1} [24]. Furthermore, the concentrations of DNA species in strand displacement systems are typically on the order of 10 nM – 1 μM. For a bimolecular rate constant $k = 5 \times 10^{-5}$ M^{-1} s^{-1} and an initial concentration of $[X]_0 = 5$ nM, the distance travelled by a wave front in 40 hours is approximately 4.55 cm, which agreed with simulations (Fig. 3a,e).

Several previous works have demonstrated the implementation of autocatalytic behaviours using DNA strand displacement [17, 27]. However, the spatiotemporal dynamics of this simple circuit has not yet been reproduced experimentally. While the wave-speed of the single reaction can be analytically characterised, the impact of diffusion and consumption of ndsDNA gates can only be predicted via numerical simulation. To address this, we compared simulations of the high-level autocatalytic reaction (3) in one spatial dimension with equivalent simulations of strand displacement implementations. Here we use a model of the autocatalytic $B + X \rightarrow 2X$ circuit that is identical to the model in [17] (Fig. 2).

We analysed spatiotemporal dynamics of the autocatalytic circuit from [17]. In an ideal parameterisation, in which all rates of toehold-mediated strand displacement are equal, we observed a very similar pattern to the CRN model (Fig. 3a,b,e). When using the experimentally calibrated rates from [17], we also found a similar pattern in the absence of leaks (Fig. 3c,e). However, approximately 1% leak from the Join$_{BX}$ gate completely disrupted the travelling wave (Fig. 3d). The strong impact of leaks on spatiotemporal dynamics is analogous

**a** Initial molecules
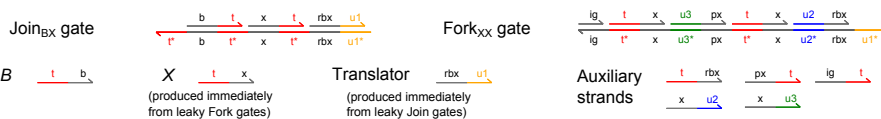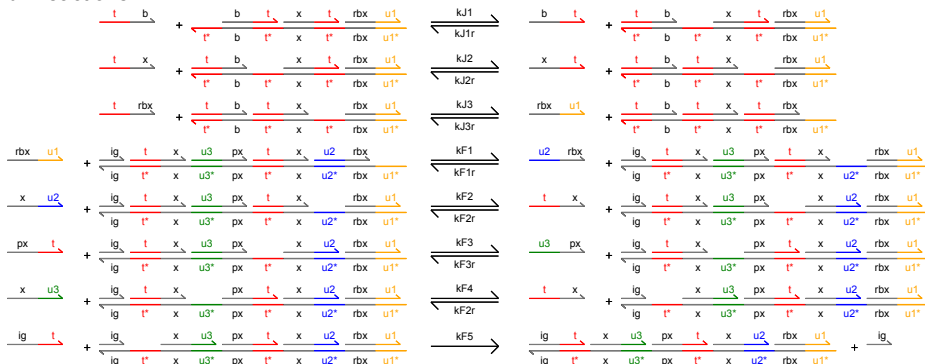
b Reactions

Fig. 2. DNA strand displacement implementation of an autocatalytic reaction. Two-domain signals and gates were used to implement the formal reaction $B + X \rightarrow 2X$, where B is the $\langle$t b$\rangle$ strand, and X is the $\langle$t x$\rangle$ strand. (a) The initial molecules are shown, including products of fast leak reactions, which are assumed to immediately produce gate outputs. (b) Complete reaction list. The reaction rates are quantified in [17], in which each rate was inferred from experimental data.

to its impact on purely temporal dynamics of autocatalytic circuits, observed in [17, 27], in which the presence of a small concentration of reactant kick-starts autocatalysis and eventually consumes all available gates. Here, as there are gates across the whole spatial domain, the presence of leaks means that diffusion from neighbouring locations is not required to kick-start autocatalysis, and so a travelling wave is not observed.

3.2 Periodic Travelling Waves in Lotka-Volterra Predator-Prey Oscillators

To analyse more complex spatiotemporal dynamics in an equivalent experimental setup, we considered designs for generating *periodic* travelling waves. Mathematical theory dictates that periodic travelling waves can be produced in spatially heterogeneous settings (i.e. with diffusion) when the corresponding spatially homogeneous dynamics show oscillations [2]. A range of CRN oscillators have been studied, providing an extensive set of examples to test. Among them, the Lotka-Volterra system is a canonical example of nonlinear dynamics, which has also been studied in the context of DNA strand displacement [15]. A Lotka-Volterra network can be described by

$$X \xrightarrow{k_1} 2X \qquad X + Y \xrightarrow{k_2} 2Y \qquad Y \xrightarrow{k_3} \varnothing \qquad (4)$$
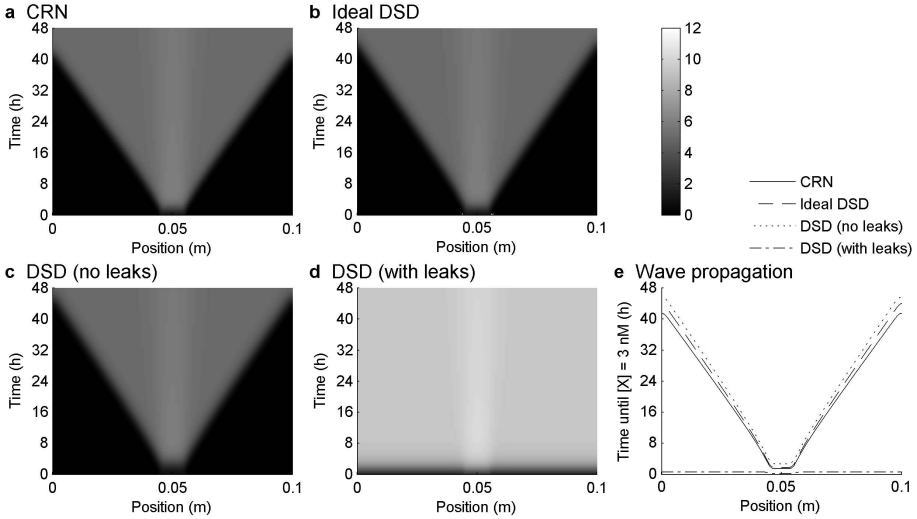
Fig. 3. Wave propagation in autocatalytic circuits. Simulations were carried out using vDSD for autocatalytic circuits. (**a**) CRN model with $k = 5 \times 10^{-5}$ nM^{-1} s^{-1}. (**b**) *Ideal* strand displacement implementation, in which all toehold-mediated strand displacement reactions occur at rate 10^{-4} nM^{-1} s^{-1}. (**c,d**) Strand displacement implementation of $B + X \rightarrow 2X$ in [17], where rates of toehold-mediated strand displacement were set to values inferred from experimental data. Leak parameters were either equal to zero (c), or at inferred quantities (d). In all cases, simulations were initialised with 1 nM of X in a central channel of width 0.01 m, and 5 nM of Y across the whole 0.1 m domain. In strand displacement models, 200 nM of gates and auxiliary strands were also supplied homogeneously. The concentration of X is indicated by the colour bar in the upper right, in nM units. (**e**) Wave propagation was characterised by determining the time at which the concentration of X reached 3 nM, half of the maximal level in the ideal system, for each point in space.

DSD Implementation of a Lotka-Volterra Predator-Prey System. To assess experimentally feasible designs for Lotka-Volterra oscillators, we translated the reactions (4) into a two-domain DNA strand displacement system (Fig. 4). In this design, the majority of toeholds are the same (domain t), though a second toehold sequence (domain u) specifically distinguishes translator strands from other single-stranded DNA strands in the system. A single toehold scheme is presented in Appendix C, where it is noted that auxiliary strand reuse (crosstalk) between gates complicates the selection of their initial concentrations.

Not all auxiliary strand crosstalk is removed in this design, as the $\langle$x t$\rangle$ strand required to release the second output on the Fork$_{2X}$ gate is also a *reverse* strand on Join$_{XY}$ gates. Thus, the effective rate constant for $X + Y \rightarrow 2Y$ may increase as Fork$_{2X}$ gates are consumed. An optimisation of this design would therefore be to remove this crosstalk.

a Initial molecules
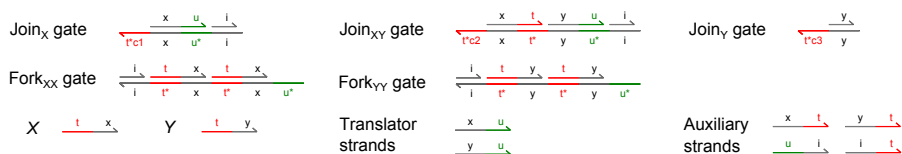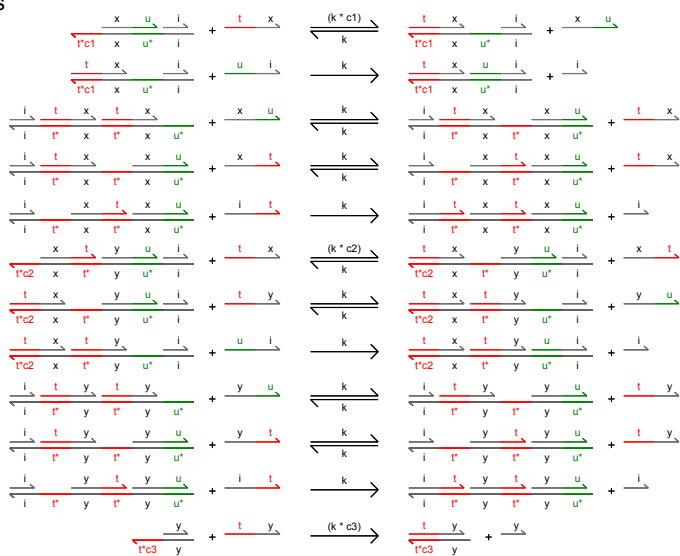
b Reactions

Fig. 4. Candidate DNA strand displacement implementation of a Lotka-Volterra oscillator. Two-domain signals and gates were used to implement the reaction system (4), where X is the $\langle$t x$\rangle$ strand and Y is the $\langle$t y$\rangle$ strand. (**a**) The initial molecules required. (**b**) Complete reaction list. The reaction rates are all set as k except for the binding of the first input strands to Join gates, which include a coefficient representing possible manipulations to the degree of complementarity. Specifically, $k_{\text{JoinX}} =$ c1*k, $k_{\text{JoinXY}} =$ c2*k, and $k_{\text{JoinY}} =$ c3*k.

Generating Oscillatory Behaviours by Modulating External Toehold Binding Rates. In order to generate periodic travelling waves, we sought conditions under which DSD versions of the Lotka-Volterra reactions gave oscillatory behaviours. Despite the potential for modulating effective rate constants by varying concentrations of auxiliary strands, we found no regime in which more than a single oscillation could be observed (simulations not shown). Instead, we considered modifications to the binding sites of inputs on the join gates, in order to obtain direct control over the effective rate constant. By shortening the sequence of the exposed toehold and thus the degree of complementarity, strand displacement reactions can be slowed down by several orders of magnitude [28]. Manipulating the rate constants in this way is equivalent to the approach in [15], in which the first step of the implementation of the bimolecular reaction is 3 orders of magnitude slower than the unimolecular reactions.

To determine an appropriate parameter regime for oscillatory behaviours, we simulated combinations of $(k_{JoinX}, k_{JoinXY}, k_{JoinY})$, where k_G is the binding of the input to gate $G \in \{JoinX, JoinXY, JoinY\}$, and analysed the resulting traces for the number of turning points within 96 h. A fixed duration was important to rule out slow yet persistent oscillations, which would be challenging to observe experimentally. Also, as gates are consumed, both the amplitude and frequency of oscillations will diminish over time, meaning it was important to use a methodology suitable for damped oscillations. Reducing binding rates to $Join_X$ and $Join_Y$ gates led to a dramatic improvement in oscillatory behaviours (Fig. 5). A reduction of approximately 2 orders of magnitude was optimal (see leftmost panels of Fig. 5a,b), and produced up to 10 turning points in the 96 h window. Reducing k_{JoinXY} led to fewer turning points in both $\langle t\ x \rangle$ and $\langle t\ y \rangle$ traces (Fig. 5c,d). The strong dependency of oscillatory behaviours on specific values of the parameters emphasises the importance of accurate quantification of these rates.
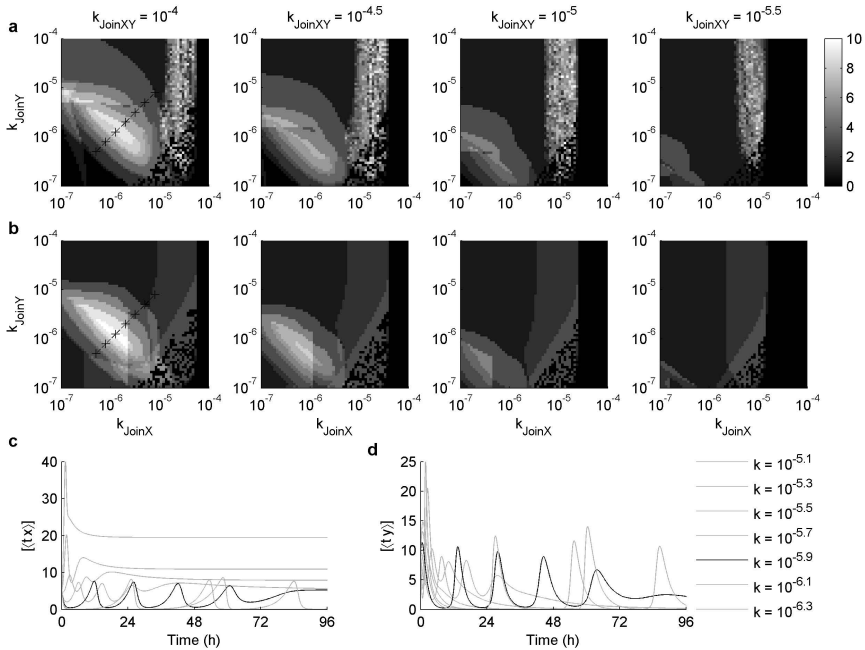
Fig. 5. Parameter analysis for the proposed DSD implementation of a Lotka-Volterra oscillator. Simulations were performed over different combinations of rates for inputs binding join gates. The simulations of (**a**) $\langle t\ x \rangle$ and (**b**) $\langle t\ y \rangle$ were analysed for the number of turning points in 96 h. (**c,d**) Example simulations corresponding to the black crosshairs in the leftmost panels of a and b. Here, $k_{JoinXY} = 10^{-4}\ nM^{-1}s^{-1}$, the values for both k_{JoinX} and k_{JoinY} are as indicated in the legend, and all other rates of toehold-mediated strand displacement were assumed to be $10^{-4}\ nM^{-1}s^{-1}$. All gates and auxiliary strands were initialised at 200 nM, and $\langle t\ x \rangle$ and $\langle t\ y \rangle$ were initialised at 10 nM.

Spatiotemporal Dynamics for Strand Displacement Oscillators. Having established parameter regimes for DNA strand displacement implementations in which oscillatory behaviour persists over 96 hours, we sought to determine whether periodic travelling wave phenomena could be produced. In addition to the consumption of gates diminishing oscillatory behaviour, we would expect the diffusion of all DNA molecules to spatially homogenise behaviours that are more heterogeneous in the CRN version. We simulated invasions of ⟨t x⟩ and ⟨t y⟩ strands in media containing the gates and auxiliary strands. We selected a parameterisation in which non-spatial simulations predicted robust cycling with minimal amplitude decay (Fig. 6a). In 1d, we observed periodic travelling waves, though the waves both decayed in amplitude and decoupled from cycles in the centre (Fig. 6b). In 2d, we observed a similar pattern, with the emergence of several travelling waves with decaying amplitude (Fig. 6c).
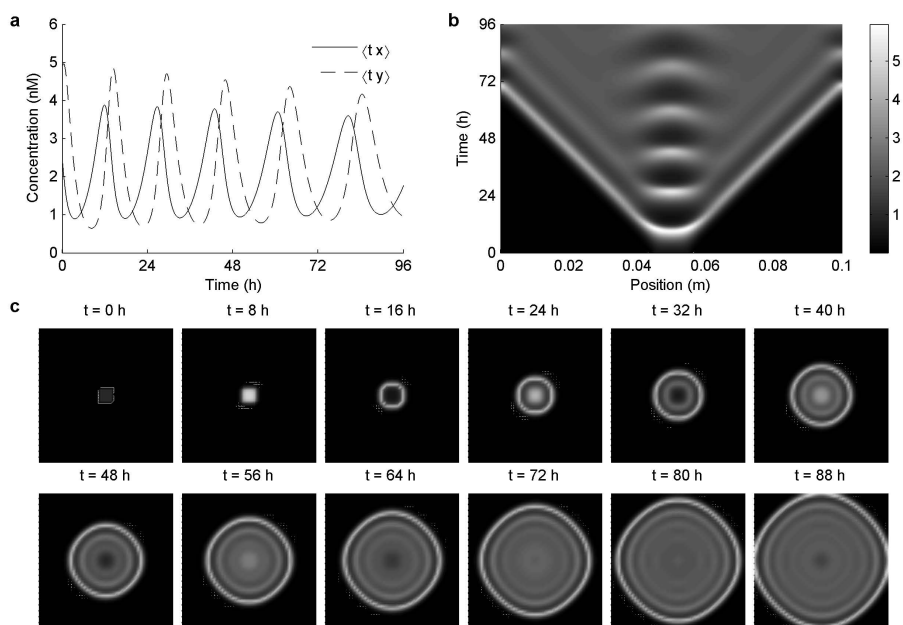
Fig. 6. Spatiotemporal dynamics of the proposed DSD implementation of a Lotka-Volterra oscillator. This DSD implementation was simulated in vDSD using parameter values identified in Fig. 5 as leading to oscillatory dynamics. Specifically, $k_{JoinX} = k_{JoinY} = 2 \times 10^{-6}$ nM^{-1} s^{-1}, and all other toehold-mediated strand displacement rates at $k = 10^{-4}$ nM^{-1} s^{-1}. (**a**) Simulation of the spatially inhomogeneous problem. (**b**) Simulation of spatiotemporal dynamics in 1d. (**c**) Simulation of spatiotemporal dynamics in 2d. In b,c, the domain was 0.1 m wide, and the solver used 101 grid-points. A central core of relative width 0.1 was applied to ⟨t x⟩ and ⟨t y⟩, 1 nM internally and 0 nM externally. All gates and auxiliary strands were supplied uniformly at 200 nM. In b and c, the concentration of ⟨t x⟩ is indicated by the colour bar in the upper right, in nM units.

Similar analysis applied to the single toehold DSD implementation revealed greater amplitude loss in non-spatial simulations, and equivalently weaker travelling waves in both 1d and 2d simulations (Fig. S3).

### 3.3 Emergence of Stationary Patterns from a Consensus Network

In previous sections, we predicted that non-stationary spatial patterns could be generated from invasion scenarios. However, owing to technical challenges in producing such initialisations in an experiment, here we considered pattern formation that only relies on inherent random spatial heterogeneity. We considered circuits with bistable dynamics, which might give rise to spatial bistability, and thus stationary patterns. Consensus algorithms use bistability to enable distributed agents holding a mixture of beliefs to reach consensus. For a binary belief, X or Y say, it is possible for a population of N agents to reach consensus on the initial majority in $O(N \log N)$ steps [29]. There are several ways to describe the algorithm in terms of chemical reaction networks (CRNs). Here, we consider the three reaction scheme

$$X + Y \xrightarrow{k} 2B \qquad B + X \xrightarrow{k} 2X \qquad B + Y \xrightarrow{k} 2Y, \qquad (5)$$

as previously implemented using two-domain strand displacement [17]. This scheme was also used in a recent analysis of consensus algorithms in a spatial context [30].

Simulation of Spatiotemporal Dynamics for the Consensus Network. To gain insight into how diffusion of DNA molecules might modulate consensus dynamics in a spatially heterogeneous experimental system, we simulated consensus networks in vDSD. As with the autocatalytic circuits in Section 3.1, we compared the spatiotemporal dynamics of the CRN level model with those from strand displacement-level models. To encode the more realistically achievable experimental setting of providing a target concentration uniformly in space, but subject to spatial variations, we used the *random* option of the spatial initial condition directive (see Table S1).

We found that consensus networks routinely produced spatial patterns in 1d within 2 days (Fig. 7). As predicted from theory [31, 32], the CRN model produced a variety of patterns that depended on the random initial configuration of the concentrations of X and Y molecules, and were demonstrably stable in time (Fig. 7a). Furthermore, these patterns were reasonably robust to deviations from a zero majority, as seen by varying $[X]$ both above and below the value of $[Y]$ (Fig. 8). We next simulated the DSD version of the consensus network, described in [17]. This network has a majority threshold that is not 1:1, owing to differences in the effective rate constants of the two autocatalytic reactions. Simulations of random perturbations to $[X] = 7.5$ nM and $[Y] = 5$ nM led to the emergence of patterns that persisted in excess of 10 days, similar to the CRN model, both in the absence (Fig. 7b) and presence (Fig. 7c) of fast leaks arising from dysfunctional dsDNA gates or ssDNA strands. The presence of leaks increased the maximum concentration of $[X]$ considerably as compared with the
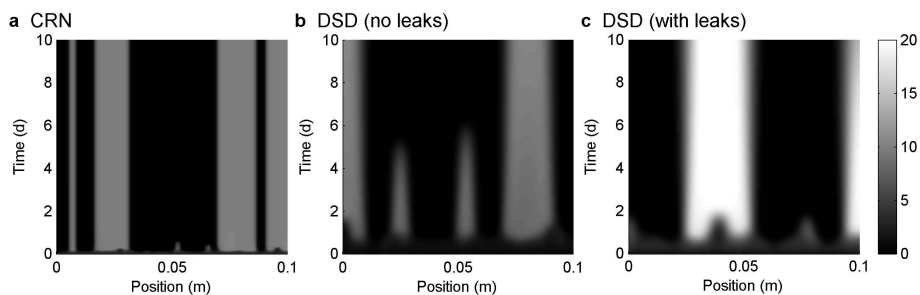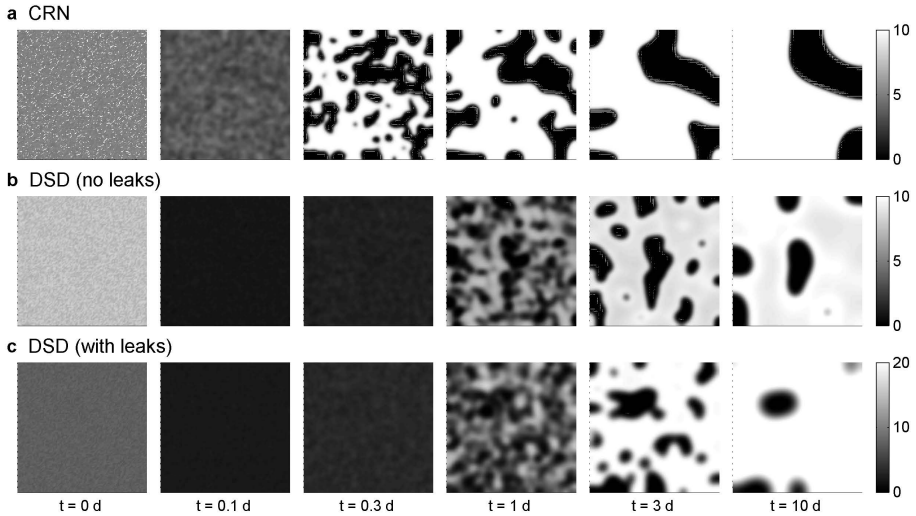
Fig. 7. Pattern formation in 1d for diffusive consensus networks. Simulations were carried out using vDSD for 1d domains. (**a**) The CRN version of the consensus network (5) was simulated with $[X]$ and $[Y]$ initialised with random perturbations to 5 nM of strength 0.2 (see Appendix A) at each grid-point. (**b**) DSD version of the consensus network assuming no leaks. (**c**) DSD version of the consensus network assuming leak parameters as quantified in [17]. The concentration of X is indicated by the colour bars on the right, in nM units.
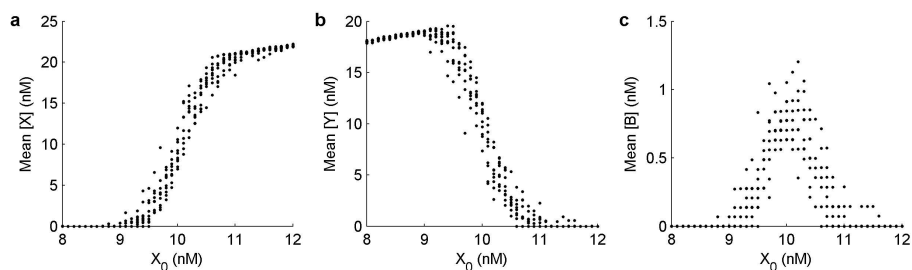

Fig. 8. Robustness of stationary patterns to initial conditions. The reaction-diffusion equations were solved for the CRN version on a 0.1 m 1d grid of 101 points, analogous to Fig. 7. Using the *random* option for the spatialic directive, initial conditions were random perturbations from $[Y] = 10$ nM and $[X]$ as indicated on the horizontal axes. Simulations were conducted 10 times each with $[X]$ initialised over 0.1 nM increments between 8 nM and 12 nM. After 20 days of simulation, the mean average of concentrations for (**a**) X, (**b**) Y and (**c**) B was computed over the domain. When the mean concentration of X is 0, this indicates that no stationary pattern was observed, and similarly when the mean of $[X]$ is equal to $10 + X_0$. Mean concentrations in between these values indicate the presence of stationary patterns. This illustrates how robustly deviations from the unstable coexistence state can be stabilised by diffusion.

CRN or DSD system without leaks, though gave qualitatively similar patterns in the same spatial domain.

Spatial patterns were also observable in 2d domains (Fig. 9). Starting from a random initial configuration of the concentrations of X and Y molecules, patterns with high amplitude emerged within 1 day of simulated time in CRN (Fig. 9a), and DNA strand displacement (Figs. 9b,c) models. As for 1-dimensional simulations, leaks did not change the qualitative behaviour of the patterns,

a CRN

b DSD (no leaks)

c DSD (with leaks)

t = 0 d   t = 0.1 d   t = 0.3 d   t = 1 d   t = 3 d   t = 10 d

Fig. 9. Pattern formation in 2d for diffusive consensus networks. Simulations were carried out using vDSD for 2d domains. (**a**) The CRN version of the consensus network (5) was simulated with $[X]$ and $[Y]$ initialised with random perturbations to 5 nM at each grid-point. (**b**) DSD version assuming no leaks. (**c**) DSD version assuming leak parameters as described and quantified in [17]. The concentration of X is indicated by the colour bars on the right, in nM units.
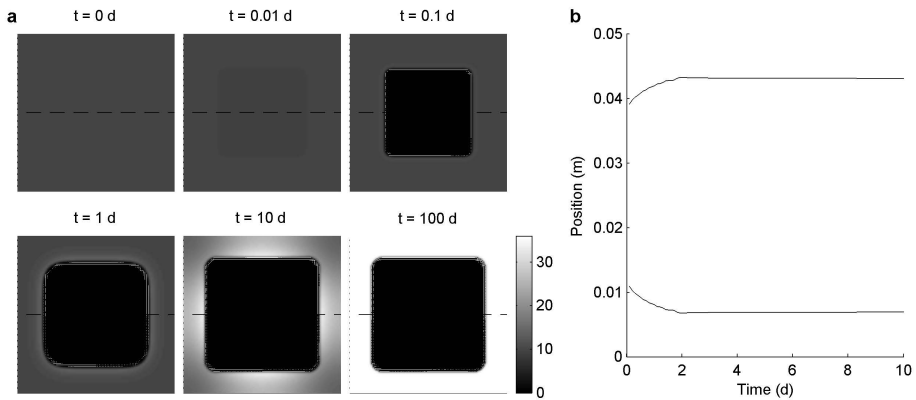
Fig. 10. Stationary pattern for the consensus network in a 2d domain. The CRN version of the consensus network (5) was simulated using vDSD, using the CRN tab, on a 0.05 m x 0.05 m grid with 101 points in each dimension. The initial conditions were set to $[Y] =$ 10 nM uniformly, and $[X] = 100$ nM in a central square of size 0.025 m x 0.025 m. (**a**) The time-evolution of $[Y]$ at times specified above each panel. (**b**) The horizontal position at which $[Y] = 5$ nM at each time-slice, at the middle of the vertical axes (indicated by dashed lines in a).

though increased the maximum concentration of X strands throughout. However, in contrast to 1d, we found that the patterns gradually disappeared over time (up to 10 days from the start of the simulated experiment). This might be due to an increased directional effect of diffusion in 2d, though could not be corrected for by reducing the rate of diffusion (simulations not shown). However, we found that stationary patterns could arise in 2d problems in invasion scenarios, in which invading species X were placed at the centre of a spatially homogeneous concentration of Y (Fig. 10). In simulations of the CRN model, a wave separating regions of high [X] from high [Y] transiently moved position, though became spatially stable by 2 days of simulated time (Fig. 10). These contrasting behaviours emphasise the importance of initial conditions on pattern formation in an experimental setting.

4 Discussion

In this article, we have shown that purely DNA-based circuits have great potential for producing spatial patterns. By using an experimentally demonstrable strategy for mapping CRNs to DNA strand displacement circuits, we provide realistic analysis of emergent spatiotemporal dynamics in the presence of isothermal diffusion. Specifically, we find that strand displacement realisations of autocatalytic circuits are particularly sensitive to leaks, which completely disrupt wave propagation. Additionally, diffusion degrades periodic travelling waves emanating from a strand displacement realisation of the Lotka-Volterra predator-prey network. However, we find that the consensus network in [17] produces stationary and travelling waves in different scenarios, both of which are robust to the presence of leaks. More generally, our simulations demonstrate that it is possible to exploit chemical diffusion to produce emergent pattern formation at the centimetre scale. The formation of patterns at this scale could open up new opportunities for programmed self-assembly.

The ability to design robust DNA-based circuits in the presence of unplanned interactions is a fundamental problem in molecular programming. While we expect DNA synthesis methods to improve over time, there will likely always be some imperfections. Therefore, the ability to both experimentally characterise and model leaks will continue to be important for fine-tuning DNA circuits. We found that leaks had varying impacts on emergent pattern formation. Autocatalytic circuits were particularly sensitive (Fig. 3a), while the consensus network was qualitatively robust (Figs. 7 & 9).

To experimentally observe the spatial patterns presented here, we note several challenges. To reproduce the scenarios in Figs. 3 and 6b,c, input DNA strands will need to be applied in a specific sub-region of the media. However, pipetting will likely result in a disturbance that will produce a travelling wave in the fluid, which might disrupt the diffusion of the DNA molecules within the solution. Therefore, pattern formation arising from more spatially uniform initial conditions is likely to be easier to achieve. In Figs. 7 and 9, initial conditions were set to be random perturbations from a target concentration, which models the inevitable spatial heterogeneity in a mixture.

Our approach to analysing DNA strand displacement circuits in the presence of diffusion has involved the extension of the Visual DSD software to describe and simulate reaction-diffusion equations. This has allowed us to conveniently analyse the dependence of spatiotemporal dynamics on different DNA gate designs, unplanned DNA interactions, fluctuations in initial conditions and kinetic rates. Future extensions could include the specification of irregular domains and a range of boundary conditions, which could be important for applications of DNA-based patterning or for describing experimental systems such as microchemostats, which involve measuring molecular interactions in chambers subjected to fluxes of reactants.

It is hoped that our methodology and corresponding software implementation will provide the means to design strand displacement circuits that both acknowledge and take advantage of the inherent spatial heterogeneity in physical systems.

References

1. Hagan, M.F., Chandler, D.: Dynamic pathways for viral capsid assembly. Biophysical J. 91, 42–54 (2006)
2. Murray, J.D.: Mathematical biology. Springer (2003)
3. Sheth, R., Marcon, L., Bastida, M.F., Junco, M., Quintana, L., Dahn, R., Kmita, M., Sharpe, J., Ros, M.A.: Hox genes regulate digit patterning by controlling the wavelength of a turing-type mechanism. Science 338, 1476–1480 (2012)
4. Reif, J., Chandran, H., Gopalkrishnan, N., LaBean, T.: Self-assembled DNA nanostructures and DNA devices. In: Cabrini, S., Kawata, S. (eds.) Nanofabrication Handbook, pp. 299–328. CRC Press, Taylor and Francis Group, New York (2012)
5. Winfree, E., Liu, F., Wenzler, L.A., Seeman, N.C.: Design and self-assembly of two-dimensional DNA crystals. Nature 394, 539–544 (1998)
6. Um, S.H., Lee, J.B., Park, N., Kwon, S.Y., Umbach, C.C., Luo, D.: Enzyme-catalysed assembly of DNA hydrogel. Nat. Mater. 5, 797–801 (2006)
7. Zaikin, A., Zhabotinsky, A.: Concentration wave propagation in two-dimensional liquid-phase self-oscillating system. Nature 225, 535–537 (1970)
8. Bauer, G., McCaskill, J., Otten, H.: Traveling waves of in vitro evolving RNA. Proc. Natl. Acad. Sci. 86, 7937–7941 (1989)
9. Isalan, M., Lemerle, C., Serrano, L.: Engineering gene networks to emulate Drosophila embryonic pattern formation. PLoS Biology 3, e64 (2005)
10. Simpson, Z.B., Tsai, T.L., Nguyen, N., Chen, X., Ellington, A.D.: Modelling amorphous computations with transcription networks. J. R. Soc. Interface 6(suppl. 4), S523–S533 (2009)
11. Padirac, A., Fujii, T., Estvez-Torres, A., Rondelez, Y.: Spatial waves in synthetic biochemical networks. J. Am. Chem. Soc. 135, 14586–14592 (2013)

12. Chirieleison, S.M., Allen, P.B., Simpson, Z.B., Ellington, A.D., Chen, X.: Pattern transformation with dna circuits. Nat. Chem. 5, 1000–1005 (2013)
13. Allen, P.B., Chen, X., Simpson, Z.B., Ellington, A.D.: Modeling scalable pattern generation in dna reaction networks. Natural Computing, 1–13 (2012)
14. Scalise, D., Schulman, R.: Designing modular reaction-diffusion programs for complex pattern formation. Technology 2, 55–66 (2014)
15. Soloveichik, D., Seelig, G., Winfree, E.: Dna as a universal substrate for chemical kinetics. Proc. Natl. Acad. Sci. 107(12), 5393–5398 (2010)
16. Cardelli, L.: Two-domain DNA strand displacement. Math. Struct. Comput. Sci. 23(02), 247–271 (2013)
17. Chen, Y.J., Dalchau, N., Srinivas, N., Phillips, A., Cardelli, L., Soloveichik, D., Seelig, G.: Programmable chemical controllers made from DNA. Nat. Nanotechnol. 8, 755–762 (2013)
18. Phillips, A., Cardelli, L.: A programming language for composable DNA circuits. J. R. Soc. Interface 6 (suppl. 4), S419–S436 (2009)
19. Lakin, M.R., Youssef, S., Polo, F., Emmott, S., Phillips, A.: Visual DSD: a design and analysis tool for DNA strand displacement systems. Bioinformatics 27, 3211–3213 (2011)
20. Qian, L., Winfree, E.: Scaling up digital circuit computation with DNA strand displacement cascades. Science 332, 1196–1201 (2011)
21. Qian, L., Winfree, E., Bruck, J.: Neural network computation with DNA strand displacement cascades. Nature 475, 368–372 (2011)
22. Amir, Y., Ben-Ishay, E., Levner, D., Ittah, S., Abu-Horowitz, A., Bachelet, I.: Universal computing by DNA origami robots in a living animal. Nat. Nanotechnol. (2014)
23. Smith, G.D.: Numerical solution of partial differential equations: finite difference methods. Oxford University Press (1985)
24. Stellwagen, E., Lu, Y., Stellwagen, N.C.: Unified description of electrophoresis and diffusion for DNA and other polyions. Biochemistry 42, 11745–11750 (2003)
25. Merkin, J., Needham, D.: Propagating reaction-diffusion waves in a simple isothermal quadratic autocatalytic chemical system. J. Eng. Math. 23, 343–356 (1989)
26. Fisher, R.A.: The wave of advance of advantageous genes. Ann. Eugen. 7, 355–369 (1937)
27. Zhang, D.Y., Turberfield, A.J., Yurke, B., Winfree, E.: Engineering entropy-driven reactions and networks catalyzed by DNA. Science 318, 1121–1125 (2007)
28. Yurke, B., Mills Jr., A.P.: Using DNA to power nanostructures. Genet. Program. Evol. M 4, 111–122 (2003)
29. Angluin, D., Aspnes, J., Eisenstat, D.: A simple population protocol for fast robust approximate majority. Distrib. Comput. 21, 87–102 (2008)
30. Lakin, M.R., Stefanovic, D.: Pattern formation by spatially organized approximate majority reactions. In: Ibarra, O.H., Kari, L., Kopecki, S. (eds.) UCNC 2014. LNCS, vol. 8553, pp. 254–266. Springer, Heidelberg (2014)
31. Gardner, R.A.: Existence and stability of travelling wave solutions of competition models: A degree theoretic approach. J. Differential Equations 44, 343–364 (1982)
32. Kan-on, Y.: Global bifurcation structure of positive stationary solutions for a classical Lotka-Volterra competition model with diffusion. Japan J. Indust. Appl. Math. 20(3), 285–310 (2003)